AD-A278 621

REP ‖‖‖‖‖‖‖‖‖‖‖‖‖‖

Form Approved
OMB No. 0704-0188

1a. REPORT SECURITY CLASSIFICATION	
Unclassified	

MARKINGS

2a. SECURITY CLASSIFICATION AUTHORITY	3. DISTRIBUTION/AVAILABILITY OF REPORT
2b. DECLASSIFICATION/DOWNGRADING SCHEDULE	See Title Page

DTIC ELECTE APR 26 1994 S

4. PERFORMING ORGANIZATION REPORT NUMBER(S)	5. MONITORING ORGANIZATION REPORT NUMBER(S)

6a. NAME OF PERFORMING ORGANIZATION	6b. OFFICE SYMBOL (If applicable)	7a. NAME OF MONITORING ORGANIZATION
SI Diamond Technology Inc	OHVJ8	DCMAO San Antonio

6c. ADDRESS (City, State, and ZIP Code)	7b. ADDRESS (City, State, and ZIP Code)
2435 North Blvd. Houston, TX 77098	615 East Houston St., P.O. Box 1040 San Antonio, TX 78294-1040

8a. NAME OF FUNDING/SPONSORING ORGANIZATION	8b. OFFICE SYMBOL (If applicable)	9. PROCUREMENT INSTRUMENT IDENTIFICATION NUMBER
ONR / SDIO	N00014	N00014-93-C-0245

8c. ADDRESS (City, State, and ZIP Code)	10. SOURCE OF FUNDING NUMBERS			
	PROGRAM ELEMENT NO.	PROJECT NO.	TASK NO.	WORK UNIT ACCESSION NO.
Code 252B RKL / Balliston Tower One 800 North Quincy St., Arlington, VA 22217-5660				

11. TITLE (Include Security Classification)

Liquid Metal Cluster Ion Source Technology for Repair of Packaging Interconnects

12. PERSONAL AUTHOR(S)
Rao Goruganthu and Howard Schmidt

13a. TYPE OF REPORT	13b. TIME COVERED	14. DATE OF REPORT (Year, Month, Day)	15. PAGE COUNT
Interim	FROM 2/1/93 TO 1/3/94	1/30/94	14

16. SUPPLEMENTARY NOTATION

17.	COSATI CODES		18. SUBJECT TERMS (Continue on reverse if necessary and identify by block number)
FIELD	GROUP	SUB-GROUP	

19. ABSTRACT (Continue on reverse if necessary and identify by block number)

Please See Page 1 of Report

94-12656
‖‖‖‖‖‖‖‖‖‖‖‖‖‖

94 4 25 068

20. DISTRIBUTION/AVAILABILITY OF ABSTRACT	21. ABSTRACT SECURITY CLASSIFICATION
☐ UNCLASSIFIED/UNLIMITED ☒ SAME AS RPT. ☐ DTIC USERS	

22a. NAME OF RESPONSIBLE INDIVIDUAL	22b. TELEPHONE (Include Area Code)	22c. OFFICE SYMBOL
Lawrence Kabacoff	703-696-0283	

DD Form 1473, JUN 86 — Previous editions are obsolete.

SECOND INTRIM REPORT
(Item No. 0001AB)

Contract Number: N00014-93-C-0245

SBIR Topic Number: SDIO 93-014

Liquid Metal Cluster Ion Source Technology for Repair of Packaging Interconnects

January 30,1994

Principal Investigator

Dr. Howard K. Schmidt
Chief Operating Officer

Accesion For		
NTIS CRA&I	☑	
DTIC TAB	☐	
Unannounced	☐	
Justification		
By _per call_		
Distribution _L Kabacoff / ONR_		
Availability Codes		
Dist	Avail and / or Special	
A-1		

SI DIAMOND TECHNOLOGY, INC.
2435 North Blvd.
Houston, TX 77098

Distribution:

> Lawrence Kabacoff, ONR, Scientific Officer
> Lambert C. McCullough, Contracting Officer
> Director, NRL
> DTIC (2 copies)
> SDIO, Attn: T/IS

SIDT Personnel:

> Dr. Howard Schmidt, PI
> Dr. Nalin Kumar, SMTS
> Dr. Mark Hammond, SMTS
> Dr. Keith Jamison, SMTS
> Dr. Rao Goruganthu, MTS

Introduction:

In this report we summarize the results of the program for writing metal features using liquid metal cluster ion source (LMCIS). We have developed a suitable source and extractor geometry for obtaining metal deposition due to charged clusters and microdroplets. The experiments were carried out using gold and lead/tin solder sources. We have carried out experiments and have characterized the quality of deposited metal/alloy films. We have evaluated throughput, spot size and shape, film adhesion to various substrates and film morhology. Experiments were also carried out to focus the charged cluster beam. Based on these results, it is feasible to apply this technology to address the problems of multi chip module integration.

1. Development of Reliable Sources

There have been essentially three different designs of LMCIS that are investigated to date. These sources are: Capillary or nozzle type, needle-nozzle type and needle type . A needle type source as shown in Figure 1, was investigated in the present study and found to produce axially symmetric distributions of cluster ions. The LMCIS source consisted of a straight tungsten rod spot welded to two tungsten wire loops. The wire loops were spot welded to two kovar pins on a ceramic base which provided mechanical support to the source. The tungsten rod was electrochemically polished to achieve a specific tip geometry and surface topography. The surface finish on the needle can be made smooth or rough by using either DC or AC voltage for electropolishing. A tip geometry that was found suitable for cluster ion emission is shown in Figure 2. A resorvoir of source material is created at the spot weld between the needle and the double wire loops. The reservoir is heated resistively by passing current through the loops to melt the source material. The liquid metal wets the needle and supplies material to the needle tip. An electric field is applied to the liquid metal surface by positively biasing the needle with respect to the extractor electrode. This field produces an eleectric field stress which pulls on the liquid film against surface tension resulting in a highly dynamic process at the liquid vacuum interface. The liquid surface deforms into a conical protrusion called Taylor cone. The onset of ion emission and formation of Taylor cone occurs at a critical voltage between the needle and the extracor. A typical voltage-current characterestics of the source is shown in Figure 3. The ion current can be varied over a wide range (1 to 300 μA) by varying the applied potential. At 50 μA of emission current a diffuse glow light in the vicinity of the apex of the needle tip. At emission currents in excess of 100 μA, deposition of gold on the substrate was achieved. At this emission current a bright

narrow beam of light originating from the neddle could be seen in the beam. At low emission currents the beam consists mainly of single and doubly charged ions while at higher emission currents cluster ions and charged micro droplets are produced. Hence cluster or micro droplet emission is required for deposition. The existence of a Taylor cone during cluster emission was documented by freezing the liquid metal by turning off the filament heater current. In Figure 4 an SEM image of the frozen Taylor cone is shown.

Stable emission currents were achieved after experimentation with fabrication of sources, extractor geometry and relative positions of the tip and extractor, filament heating current and extraction voltage. For instance, erratic emission current observed with some sources was traced to wetting problems on the needle. It was also found that position of the needle tip half way of the thickness of the extractor produced less divergence of the cluster beam.

2. Characterization of Deposited Film Properties

2.1 Throughput: A polished silicon wafer was placed a distance of 12 mm from the extractor to intercept the beam. A dektak profile of the deposited spot was obtained to find the net deposition rate at different emission currents. The profile showed net deposition and was surrounded by an etched silicon area. From the gold source, at an emission current of 160 μA a net deposition of 4 x 10^3 μm^3/s was achieved. The deposited spot was ~ 1 mm in diameter. Surrounding the central deposit was a more sharply defined annular area whose outside diameter was 20 mm. Surrounding this was another annular area resembling a halo. From the dimensions of the deposited spot and the etched area, cluster beam and ion beam divergences are computed to be 2 and 45 degrees respectively. Since during deposition simultaneous emission of ions and droplets takes place, sputter etching during deposition competes with the metal deposition due to droplets. Net deposition is observed for emission currents greater than 100 μA. This suggests that the emission current has to be greater threshold value for achieving deposition using these sources.

Throughput was also measured using Pb-sn solder material using the same tip geometry as that used for the gold source. At 150 μA of emission current, a deposition rate of 95 x 10^3 μm^3/s was observed. The higher throughput for solder as opposed to gold is perhaps due to the smaller surface tension of solder at its melting point. Emission current of upto 1 mA was observed with this source. The deposition rates obtained for this source for a series of emission currents are shown in Figure 5.

2.2 microstructure: Microstructure of the films deposited on silicon substrate at emission current of 150 uA from a gold source were studied by scanning electron microscopy. Two SEM micrographs are shown in Figures 6 (a) and 6 (b). The deposited films show fine textured structures. The grain size is of the order of 0.1 microns. These films were deposited with the substrate at room temperature. The other SEM picture indicates some splatter indicating that the droplets are not solidified as they landed on the substrate. The deposited films show some surface roughness and porosity but is still acceptable for many applications in MCM integration.

2.3 Adhesion: Adhesion of the deposited gold films using LMCIS to various substrates was investigated. We deposited gold on bare conducting polished silicon wafer, polyimide film and stainless steel. In all cases the film adhesion passed scotch tape test.

3. Focussing of the cluster ion beam:

The emitting species from the gold LMCIS include Au^+, Au^{+2}, Au_2^+ and cluster ions, Au_n^{+m} ($n>10$, $n>m$) and charged micro-droplets. Consequently, the emitting species show a large distribution of charge to mass ratios (Q/m). The focussing properties of electrostatic lenses do not depend on the charge to mass ratio of the ions and hence have been used for focussing charged particles from LMCIS sources. The virtual source size for these cluster ion source has been determined to be less than 8 microns. Hence no demagnification of the source size is necessary.instead a magnification of up to 2 is acceptable for achieving the desired feature sizes for Multi chip module (MCM) applications. The design choices for the focussing column include a two lens (projective/ objective) or a single lens column. A single lens column is easier to fabricate and align. Hence we opted for a single lens column using an asymmetric Einzel lens design as shown in Figure 7. Because of the small source size, the image spot size is limited mainly by the chromatic and spherical aberrations in the lens. The chromatic aberration limited spot size is dependent on the aberration coefficient, acceptance angle and specific energy spread (dE/E) of the beam. The aberration coefficient for the Einzel lenses is governed by the lens geometry and is a minimum when used with unity magnification. The beam energy spread is characterestic of the source. However, the aberration limited spot size varies linearly with the acceptance angle. The spot size is larger for larger acceptance angle and vice versa. The LMCIS source was found to produce cluster beam with an included emission angle of 4 degrees. Use of a smaller aperture is undesirable as it reduces the throughput and leads to blocking of the aperture with deposit.

Experiments were carried out with an aperture (0.81 mm dia) to limit acceptance angle to +/- 1.5 degrees. The lens ion optical properties were studied using a public domain ion optics program "SIMION". The required voltage on the middle electrode for focussing and spot size were calculated for different source to aperture and source to target distances. The required focus voltage was caculated to be 60% of the beam voltage. From these studies it is expected that a specific energy spread of 1% a beam spot size of 60 microns in diameter can be achieved. By decreasing the acceptance angle still smaller spot size can be achieved.

Although the emission source is axially symmetric it should be aligned with the optic axis of the lens to minimize other geometrical aberrations such as distortion, field curvature, astigmatism and coma. The source and extractor assembly were mounted on an XYZ manipulator and can be tilted in two orthogonal planes. An extraction voltage of 12 kV was selected and various voltages were applied to the middle electrode of the lens. For each focus voltage the beam was exposed to a clean area on the silicon wafer mounted on an XY stage to record the deposition spot. The exposure time was also recorded to determine deposition rates. In Figure 8, optical microphotographs of deposited spot for 3 different focus voltages are shown. The deposited spots are clearly distortred. A localized spot of less than 20 microns wide and 100 microns long can be seen in these pictures. An SEM image of this deposited spot is shown in Figure 9 to bring out the deposited spot. In Figure 10 various spot shapes obtained at the same focus voltage for different tilt positions of the source are shown. Clearly, the spot shape changes drastically with alignment. From these experiments it is concluded that well defined localized depositions of 50 micron features can be achieved with these lens columns by proper alignment and perhaps by reducing the acceptance angle further.

Dektak profiles of deposition spots made using focussed LMCIS beam are shown in Figures 11 (a) and 11 (b). Notice that the peak height is 1.85 and 5.5 microns in these two cases. From the exposure times and from profilometry data a deposition rate of 90 μm^3 /s was calculated. The results are summarized in Table I.

4. Evaluation of Etching capabilities

As mentioned earlier that if the LMCIS is operated at currents below 100 μA beam current, the beam consists essentially of singly charged ions and doubly charged single ions.. These ions can be focussed and used for etching any material. This phenomenon has been used extensively and described in detail in the literature. The Au ion beam produced by LMCIS is proved to produce similar etching very effectively as shown in Figure 12.

Table I. Deposition rates achieved with a focussed LMCIS beam using gold.

Deposition time (s)	height (μm)	Deposition rate (μm^3/s)	Growth rate (μm/s)
10	0.3	83	0.03
30	1.1	101	0.04
60	1.9	70	0.03
150	5.5	81	0.04

5. Evaluation of LMCIS Technology for MCM integration

The results from the studies of gold LMCIS have shown sufficient throughput, excellent adhesion, small grain size and low porosity. From the focussing results it is clear that feature sizes of 50 μm can be obtained with this technique. These factors make LMCIS technology viable for customization of MCM using spot links and cuts in the conductor traces. Even with the aberrations in the deposited spot, well defined gold features can be made by a post process step of gold etch. The profile of such a post processed deposit is shown in Figure 13.
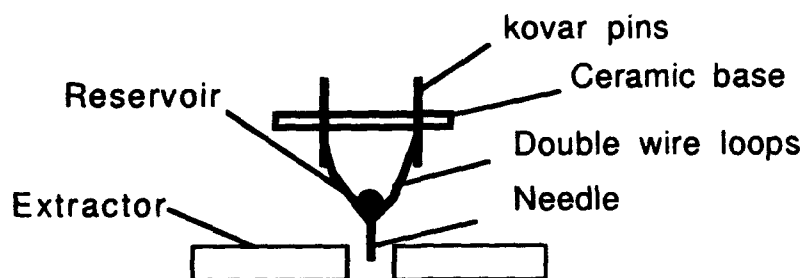
Figure 1: A schematic view of the needle type liquid metal cluster ion source.
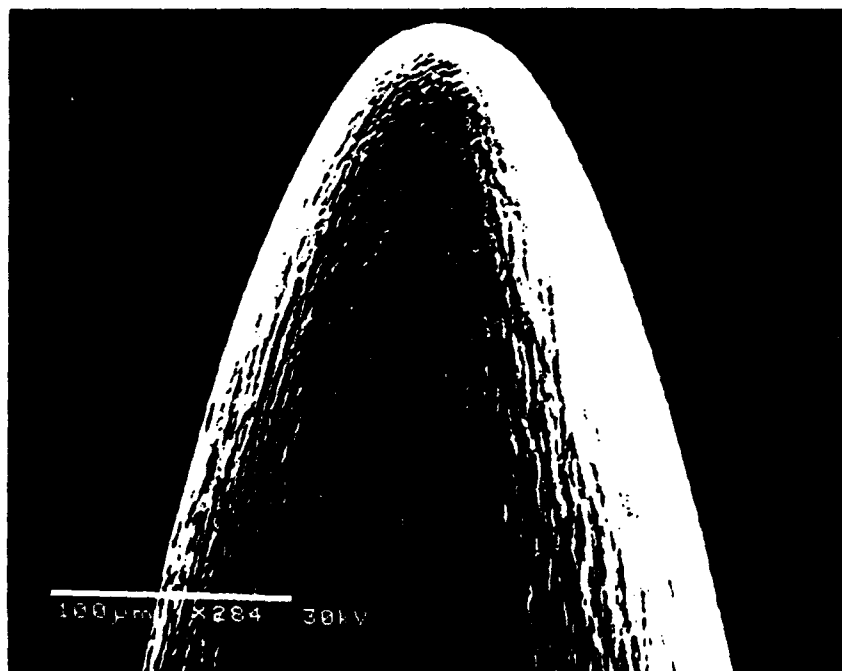
Figure 2: Tip profile of the tungsten needle of an LMCIS fabricated by electro chemical polishing. This rounded tip geometry of 40 μm tip radius produced desired emission properties. The surface roughness is desired for better flow of material to the tip.
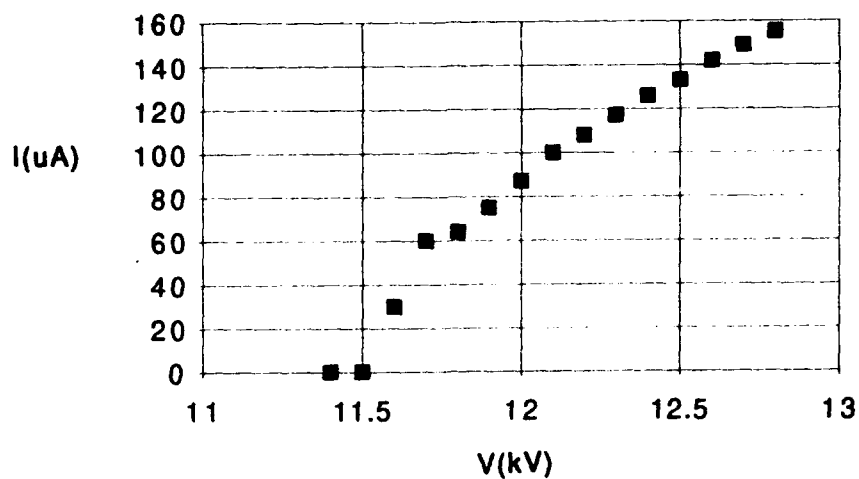
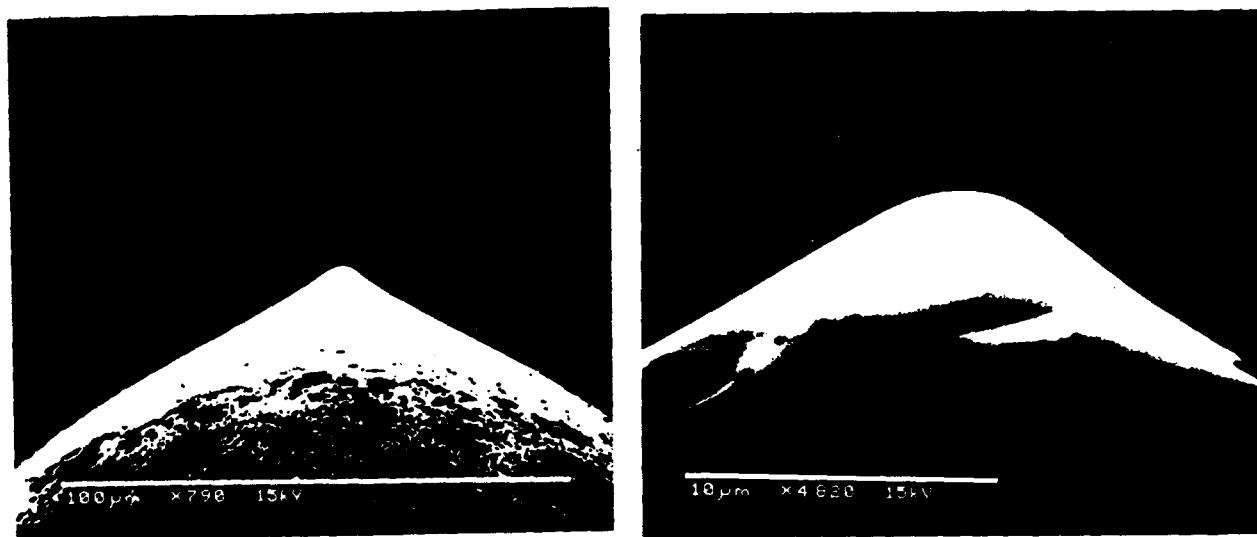Figure 3: Current voltage characterestics of a gold LMCIS. Notice the critical voltage required for the onset of field emission.

Figure 4: SEM images of the Taylor cone frozen from an operating LMCIS. The left side SEM image shows a deformed liquid metal surface quite different from the needle profile. The right side SEM image shows a close up of the apex of the Taylor cone.
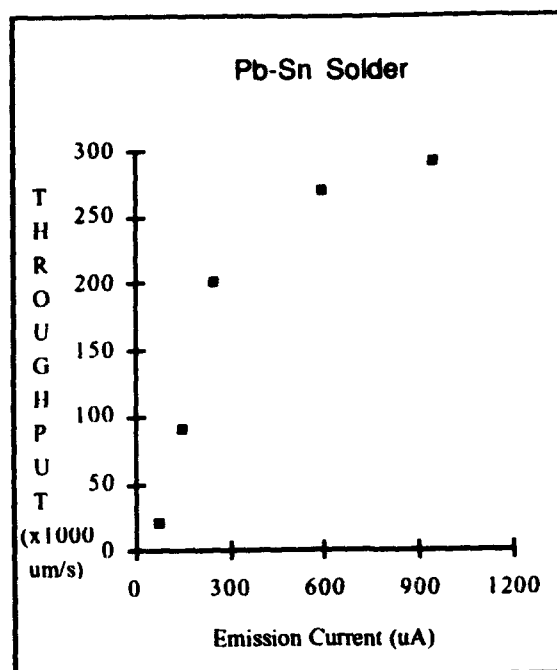
Figure 5: Throughput of an LMCIS using Pb-Sn solder
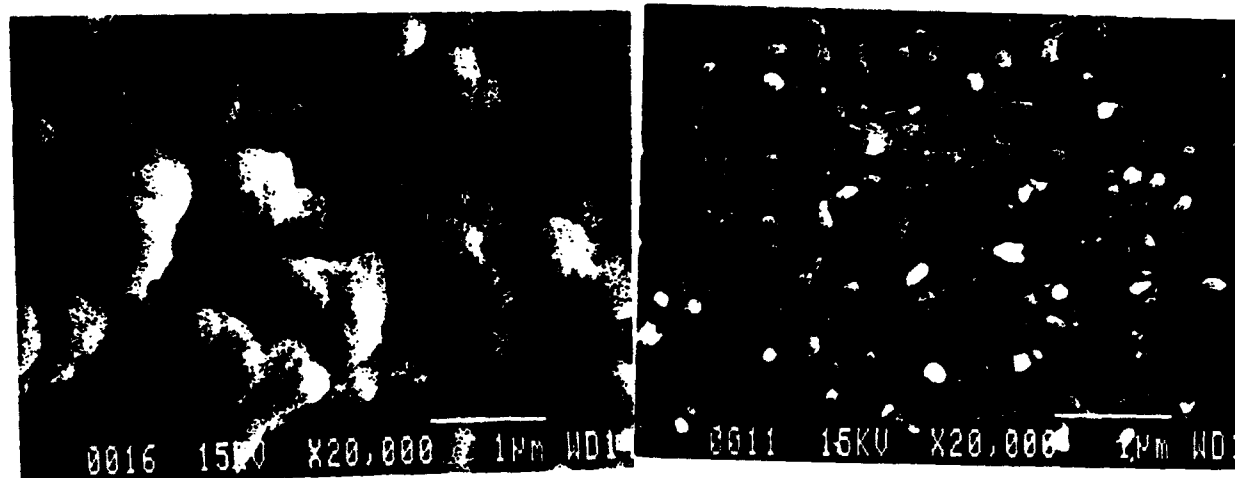
(a)   (b)

Figures 6 : SEM images of gold films deposited using LMCIS. The figure on the
left (a) shows fine grain structure of the film. On the right (b) an SEM image of
another gold film deposited at higher emission current is shown. Splatter is evident
and it might be due to large metal droplets.

LMCIS SYSTEM SCHEMATIC
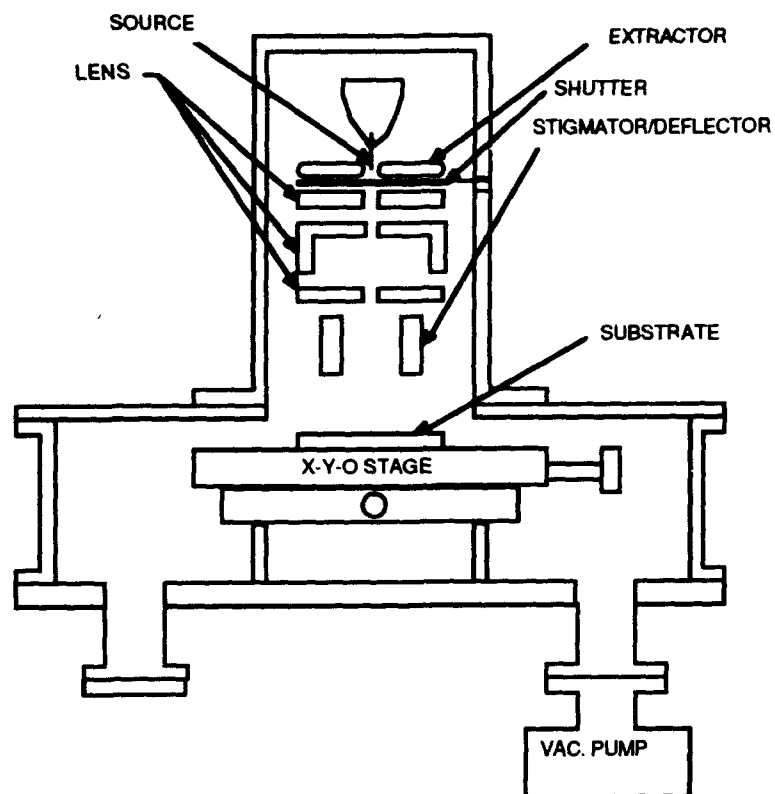
Figure 7: A schematic of LMCIS column. An asymmetric Einzel lens is used for focussing.

Figure 8: Optical microphotographs of the deposited spot on silicon wafer for lens voltages of 6.8 (top), 7.2 (middle) and 7.4 (bottom) kiloVolts. The beam energy was 12 kV. Distortions in the image are due to misalignement of the beam and lens optical axis.
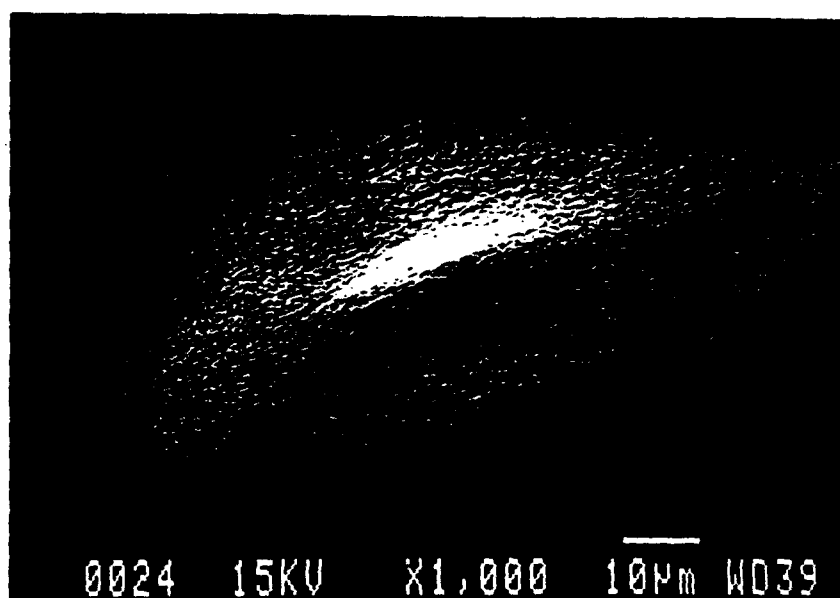
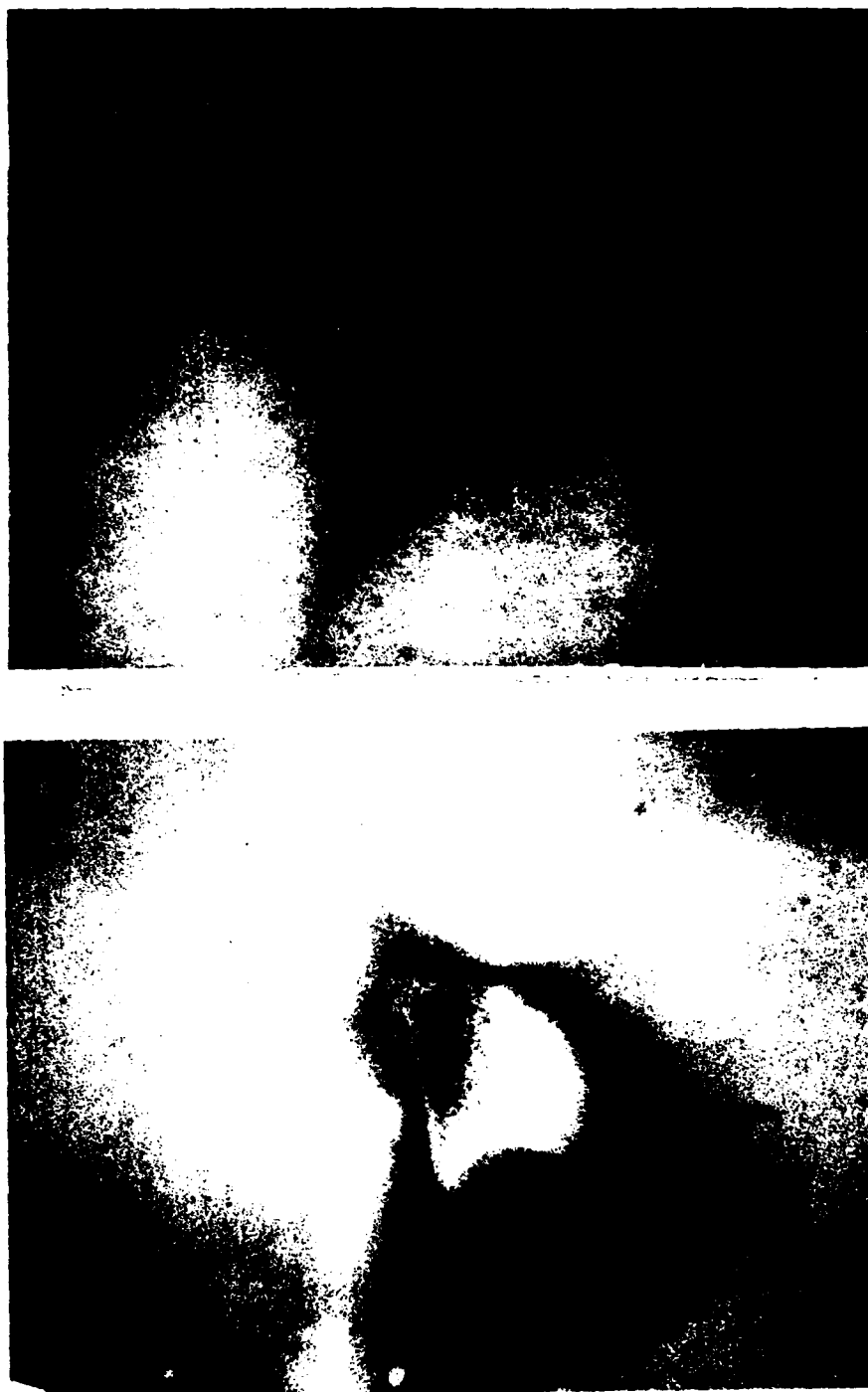Figure 9: SEM image of a deposited gold spot from focussed LMCIS beam. The central feature is 15 μm wide and 80 μm long.

Figure 10. Optical photomicrographs of deposited gold spots on silicon wafer using focussed beam of an LMCIS. The source was repositioned between these two depositions. Drastic change in the spot shape is indicative of misalignment between lens axis and beam.
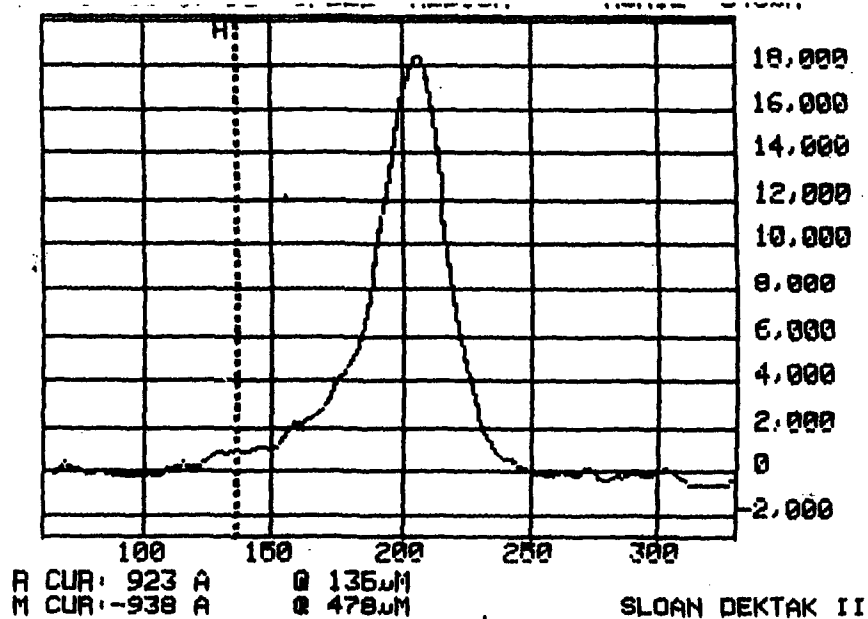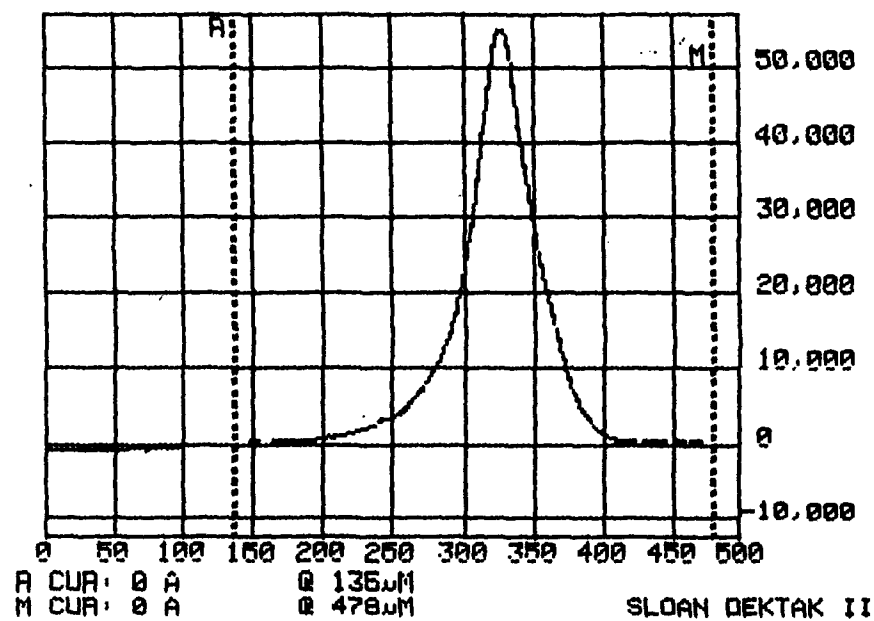
Figure 11: Dektak profiles of the deposited spot across the smaller dimension. The features are rectangular, similar to the one in Figure 9. The scanning was done across the width of the feature.
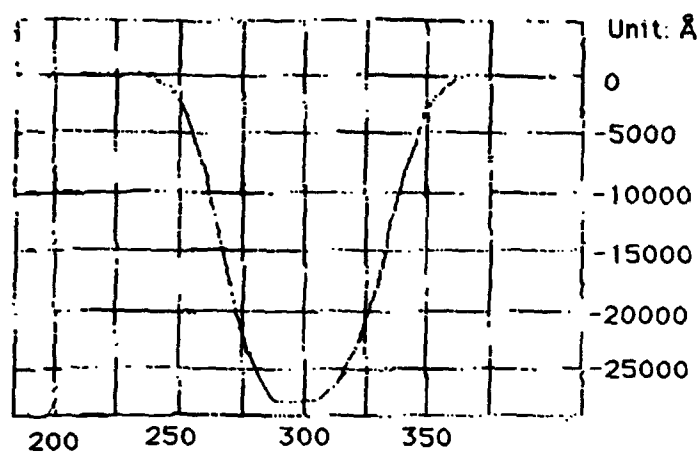
Figure 12: A 2.5 micron deep, 100 microns wide pit etched in silicon by a gold ion beam produced by LMCIS.
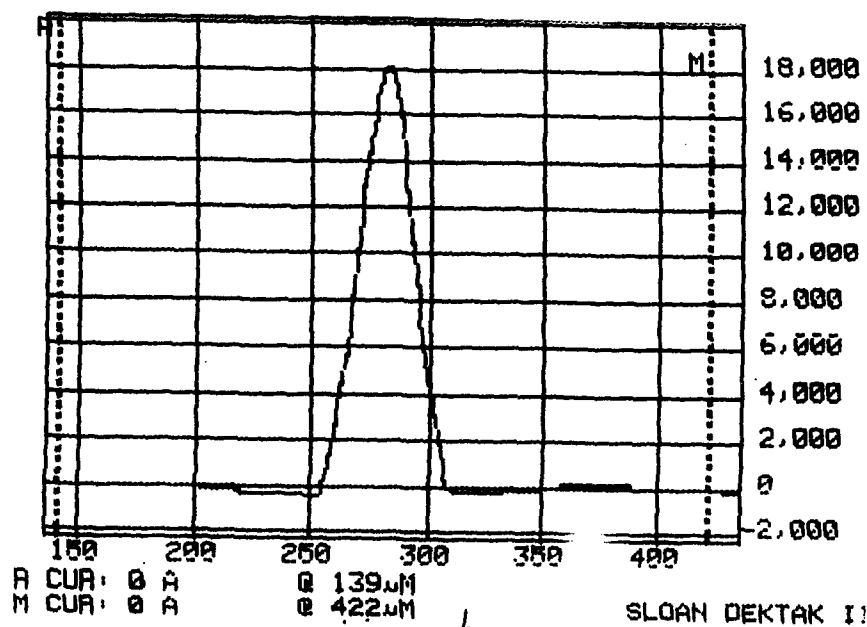

Figure 13: Dektak profile of a deposited spot using focussed LMCIS beam after a gold etch of 2000 Å   The vertical scale is in Å and horizontal scale is in microns.